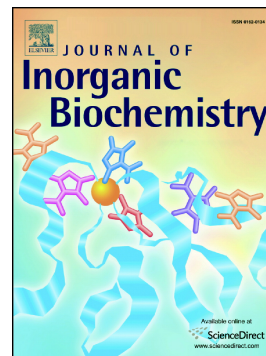


Accepted Manuscript

G-quadruplex and duplex DNA binding studies of novel Ruthenium(II) complexes containing ascididemin ligands

Maierhaba Wumaier, Jing-Jing Shi, Tian-Ming Yao, Xiao-Chun Hu, Ru-Ru Gao, Shuo Shi



PII: S0162-0134(18)30685-8
DOI: <https://doi.org/10.1016/j.jinorgbio.2019.03.021>
Reference: JIB 10681
To appear in: *Journal of Inorganic Biochemistry*
Received date: 24 November 2018
Revised date: 22 March 2019
Accepted date: 27 March 2019

Please cite this article as: M. Wumaier, J.-J. Shi, T.-M. Yao, et al., G-quadruplex and duplex DNA binding studies of novel Ruthenium(II) complexes containing ascididemin ligands, *Journal of Inorganic Biochemistry*, <https://doi.org/10.1016/j.jinorgbio.2019.03.021>

This is a PDF file of an unedited manuscript that has been accepted for publication. As a service to our customers we are providing this early version of the manuscript. The manuscript will undergo copyediting, typesetting, and review of the resulting proof before it is published in its final form. Please note that during the production process errors may be discovered which could affect the content, and all legal disclaimers that apply to the journal pertain.

**G-quadruplex and duplex DNA binding studies of novel Ruthenium(II) complexes
containing ascididemin ligands**

**Maierhaba Wumaier,^a Jing-Jing Shi,^{*b} Tian-Ming Yao,^{*a} Xiao-Chun Hu,^a Ru-Ru
Gao,^a Shuo Shi^{*a}**

^a **Shanghai Key Laboratory of Chemical Assessment and Sustainability, School of
Chemical Science and Engineering, Tongji University, Shanghai, 200092, P.R.
China**

^b **VARI/SIMM Center, Center for Structure and Function of Drug Targets, CAS-
Key Laboratory of Receptor Research, Shanghai Institute of Materia Medica,
Chinese Academy of Sciences, Shanghai 201203, P.R. China**

Corresponding author:

Shuo Shi, E-mail: shishuo@tongji.edu.cn.

Tian-Ming Yao, E-mail: tmyao@tongji.edu.cn.

Jing-Jing Shi, E-mail: shijingjing@simm.ac.cn

Abstract

In this paper, three new Ruthenium(II) polypyridyl complexes containing ascididemin (ASC) as main ligand have been synthesized and characterized. Their interactions with different G-quadruplex (Htelo, c-myc and c-kit) (Htelo: human telomeric DNA, c-myc: cellular-myelocytomatosis viral oncogene, c-kit: oncogene c-kit promoter sequences) and duplex (ds26) DNA sequences were comparatively studied with the free ligand ASC by a series of spectroscopic techniques including UV-vis (ultraviolet-visible) spectroscopy, FID (fluorescent intercalator displacement) assay, and FRET (fluorescence resonance energy transfer) melting assay. Molecular docking studies were also performed to support the binding mode of the compounds with G-quadruplex DNA. Results indicated that $[\text{Ru}(\text{bpy})_2\text{ASC}]\cdot(\text{PF}_6)_2$ (**1**), $[\text{Ru}(\text{phen})_2\text{ASC}]\cdot(\text{PF}_6)_2$ (**2**), $[\text{Ru}(\text{tatz})_2\text{ASC}]\cdot(\text{PF}_6)_2$ (**3**) (bpy = 2,2'-bipyridine, phen = 1,10-phenanthroline, tatz = 1,4,8,9-tetra-aza-triphenylene) and ASC can effectively bind G-quadruplex and duplex DNA and stabilization ability lies in the order **3** > **2** > **1** > ASC. Complex **3** was determined to be the most promising candidate for further in vitro studies and potential anticancer drug.

Keywords: Ruthenium complexes, G-quadruplex, duplex DNA, ascididemin

1. Introduction

Metalloodrugs plays an important role in cancer treatment [1]. The well-known metal based chemotherapy drug is cisplatin. But its severe side effects and drug resistance limited its application [2]. In order to overcome the drawbacks of currently used chemotherapy and find more clinically efficient anticancer drugs, several classes of alternative metal based compounds were developed [1]. Among these metal complexes, ruthenium (Ru) complexes stood out, especially because of its physiologically accessible oxidation states and lower toxicity toward healthy tissue probably due to the ability of Ru to mimicking iron in binding to biomolecules [3-5]. A number of Ru complexes showed promising anticancer activities and three of them, NAMI-A (imidazolium-trans-DMSO-imidazole-tetrachlororuthenate), KP1019 {imidazolium trans-[tetrachlorobis(1H-indazole)ruthenate(III)]} and (N)KP1339 {sodium trans-[tetrachloridobis(1H-indazole)ruthenate(III)]} have successfully entered in clinical trials [6-8].

Binding of small molecules with DNA has been studied extensively since DNA is the material of inheritance and controls the structure and function of cells [9,10]. In this respect Ru(II) complexes have attracted a great deal of attention due to their strong DNA-binding and potential anticancer activities [11-14]. Furthermore, DNA is highly polymorphic and can adopt a variety of different helical conformations [15,16] (B [17], A [18], and Z [19]) as well as unusual structures (hairpins [20], cruciform [21], triplexes [22], i-motif [23] and G-quadruplexes [24]). It has been suggested that these secondary DNA structures could be involved in the regulation of several key biological processes. Among these different non-canonical DNA motifs, DNA G-quadruplex are probably the

most extensively studied [25,26]. Such structures are made up of G-quartet subunits, where four coplanar guanines (G) are linked together by Hoogsteen hydrogen bonds [27-31]. G-quadruplex structures are highly dynamic and polymorphic too, which can fold into different topologies such as, parallel, antiparallel and hybrid depending on the base sequences, loop connectives and cations [32]. During the last decade, G-quadruplex has emerged from being a structural curiosity observed *in vitro*, to being recognized as a possible nucleic acid based mechanism for regulating multiple biological processes *in vivo* [33,34]. There is great evidence that G-quadruplexes play an overarching role in biology. G-quadruplexes are found throughout the human genome [35] and in mRNA [36], especially in gene promoters and telomeres. For example, human telomeric DNAs are made up of double stranded TTAGGG repeats and ends 3' single stranded overhang [37-40]. The folding of the single stranded 3' overhang into G-quadruplex makes the telomerase lose substrate, inhibits telomerase activity (which is up regulated more than 85% cancer cells), and prevents telomere extension, thus induces tumor cells senescence and apoptosis [40-44]. Owing to the strong relations between telomerase and cancers, great efforts have been devoted to develop the anticancer strategy based on small molecules that could target and stabilize G-quadruplex structure, with the aim of inhibit telomerase and induce cancer cell death. In addition, G-quadruplex formation in oncogene promoter regions such as c-kit (oncogene c-kit promoter sequences), c-myc (cellular-myelocytomatosis viral oncogene), bcl-2 (b-cell CLL/lymphoma 2) and K-ras (kirsten rat sarcoma viral oncogene) has been proposed to function as a transcriptional controller of these genes [45], gene expression can be suppressed by G-quadruplex stabilizing ligands [46].

Ru(II) complexes have been reported to be both duplex and G-quadruplex structure stabilizers, and potent anticancer agents [11-14]. Barton, Norden, as well as Ji groups have provided detailed information about recognition and reactions of classical duplex DNA by Ru complexes [47-50]. Over the past 15 years, a rational approach to design Ru complexes that can selectively interact with G-quadruplex DNA has emerged. For example, a series of Ru(II) complexes synthesized by our lab, have shown remarkable G-quadruplex formation and stabilization ability [51-54]. Rickling et al. studied the interactions of the dinuclear $[(\text{tap})_2\text{Ru}(\text{tpac})\text{Ru}(\text{tap})_2]^{4+}$ complex with the human telomeric sequence of $d(\text{T}_2\text{AG}_3)_4$ (tap = 1,4,5,8-tetraazaphenanthrene, tpac = tetrapyridoacridine). They found that the complex can damage these sequences by intramolecular photocrosslinking [55]. Piraux et al. reported the new Ru(II) complexes based on a novel dipyrazino [2,3-a:2',3'-h]phenazine ligand (dph), and these complexes behave as selective probes for G-quadruplex [56]. Besides, a number of Ru based on anticancer agents targeting G-quadruplex, such as, $\text{cis-}[\text{RuCl}_2(\text{S}(-)\text{-FOA})(\text{DMSO})_2]$ [57], $[\text{Ru}(\text{bpy})_2(\text{icip})]^{2+}$, $[\text{Ru}(\text{bpy})_2(\text{pdppz})]^{2+}$ and $[\text{Ru}(\text{bpy})_2(\text{tactp})]^{2+}$ [58], $(\eta^6\text{-C}_6\text{H}_6)\text{Ru}(\text{p-XPIP})\text{Cl}]\text{Cl}$ [59], $[(\text{bpy})_2\text{Ru}(\text{bpibp})\text{Ru}(\text{bpy})_2](\text{ClO}_4)_4$ and $[(\text{phen})_2\text{Ru}(\text{bpibp})\text{Ru}(\text{phen})_2](\text{ClO}_4)_4$ [60] have been reported too {FOA = 4-(2,3-dihydroxypropyl)-formamide oxoaporphine, bpy = 2,2'-bipyridine, icip = 2-(indeno[2,1-b]chromen-6-yl)-1H-imidazo[4,5-f][1,10]phenanthroline, pdppz = phenanthro[4,5-abc]dipyrido-[3,2-h:2',3'-j]phenazine, tactp = 4,5,9,18-tetraazachryseno[9,10-b]-triphenylene, X = Cl, PIP = 2-phenylimidazole[4, 5f][1,10]phenanthroline, bpibp = 4,4'-bis (1, 10-phenanthroline-[5, 6-d] imidazole-2-yl)-biphenyl, phen = 1,10-phenanthroline}.

From the previous studies, ideal G-quadruplex binder should show a high level of selectivity between quadruplex and duplex DNA when attempting to develop a powerful anticancer drug. However, anthracyclines daunomycin and doxorubicin that are two widely used anticancer drugs [61], exhibit non-selective binding properties between quadruplex and duplex DNA [62], which play an important role in their chemotherapeutic effects [63]. Experimental evidence suggests that intercalation of an anthracyclines into DNA duplex structure playing critical roles in suppressing tumor growth [64]. Besides, these drugs can also interact with telomeric DNA quadruplexes and induce cancer cell senescence and apoptosis [65]. These results hint some anticancer drugs might bind both G-quadruplex and duplex DNA.

Ascididemin (ASC) is a pentacyclic marine pyridoacridine alkaloid, which extracts from the marine animal tunicates and sponges [66-68]. Due to its significant cytotoxic properties against a series of tumor cell lines, including multidrug resistant cancer cells, ASC has received great interest [69]. It has been reported that, ASC intercalates into DNA base pairs, especially at GC-rich sequences and inhibits topoisomerase II enzyme [66-69]. Bonnard and co-workers reported that, DNA binding is the likely reason of ASC cytotoxic activity [69]. We conceive that Ru(II) complexes of ASC ligands would be a potent G-quadruplex DNA binders, as they would possess a planar aromatic ligands, which can stack on the flat surface of a terminal G-quartet in quadruplex structures.

In this study, we have combined three Ru(II) polypyridyl complexes containing N-N-chelating ligands, such as $[\text{Ru}(\text{L})_2\text{Cl}_2]$ [$\text{L} = \text{bpy}$, phen and tatp (1,4,8,9-tetra-azatriphenylene)] with ASC ligands to generate three novel complexes named $[\text{Ru}(\text{bpy})_2\text{ASC}]^{2+}$ (**1**), $[\text{Ru}(\text{phen})_2\text{ASC}]^{2+}$ (**2**) and $[\text{Ru}(\text{tatp})_2\text{ASC}]^{2+}$ (**3**), the synthetic

route to complexes **1-3** are shown in Scheme 1. In order to evaluate the quadruplex binding affinity, selectivity and structure-activity relationships of ruthenium complexes **1-3** and ASC with different DNA structures, a series of spectroscopic analysis and molecular docking studies have been carried out. In this experiment three different quadruplex sequences, including Htelo (human telomeric DNA), c-myc and c-kit that all can form G-quadruplex in the presence of K^+ condition and duplex DNA (ds26) were selected to study.

2. Experimental section

Materials. All reagents and solvents were obtained from commercial sources and used without further purification, and Ultrapure MilliQ water was used in all experiments. DNA oligomers were purchased from Sangon (Shanghai, China). Concentrations of these oligomers were determined by measuring the absorbance at 260 nm after melting. Single strand extinction coefficients were calculated from mononucleotide data using a nearest-neighbor approximation [70,71]. The formation of intramolecular G-quadruplexes were carried out as follows: the oligonucleotide samples dissolved in different buffer solutions, heated to 90 °C for 5 min, slowly cooled down to room temperature and then incubated at 4 °C overnight. The buffers were prepared as follows: (A): 10 mM tris-HCl, 100 mM KCl, pH 7.0; (B): 10 mM KH_2PO_4 - K_2HPO_4 , 100 mM KCl, pH 7.0. Stock solutions were stored at 4 °C and used after no more than 4 days. The structure of Htelo is the mixed parallel/antiparallel G-quadruplex in K^+ buffer. All of the tested compounds were dissolved in DMSO, and the concentration of DMSO was 1% (v/v).

DNA sequences

Htelo: 5'-AGGGTTAGGGTTAGGGTTAGGG-3'

c-myc: 5'-TGGGGAGGGTGGGGAGGGTGGGGAAGG-3'

c-kit: 5'-AGGGAGGGCGCTGGGAGGAGGG-3'

ds26: 5'-GTTAGCCTAGCTTAAGCTAGGCTAAC-3'

LHtelo: 5'-FAM-AGGGTTAGGGTTAGGGTTAGGG-TAMRA-3'

Lc-myc: 5'-FAM-TGGGGAGGGTGGGGAGGGTGGGGAAGG-TAMRA-3'

Lc-kit: 5'-FAM-GGGAGGGCGCTGGGAGGAGGG-TAMRA-3'

Synthesis and characterization. The compounds quinoline-5,8-dione, 1,10-phenanthroline-5,6-dione, *cis*-[Ru(bpy)₂Cl₂] \cdot 2H₂O, *cis*-[Ru(phen)₂Cl₂] \cdot 2H₂O and *cis*-[Ru(tatp)₂Cl₂] \cdot 2H₂O were synthesized according to the literature procedures [72-75]. The ligand ASC used in this work was prepared according to the literature methods [68].

[Ru(bpy)₂ ASC] \cdot (PF₆)₂ (1). Under an argon atmosphere, ASC (50.0 mg, 0.177 mmol, 1eq) and *cis*-[Ru(bpy)₂Cl₂] \cdot 2H₂O (92.0 mg, 0.177 mmol, 1eq) were mixed in EtOH:H₂O (6:1, v/v). The reaction mixture was refluxed for 6-8 h. Upon cooling, the reaction mixture was diluted with water and filtered to remove solid impurities. Then, concentrated aqueous solution of NH₄PF₆ was added to the filtrate until no more precipitate formed. The crude product precipitate filtered, dried. The dried solid product dissolved in MeCN, purified by silica chromatography eluting with MeCN: H₂O:NaNO₃ (40:4:1). This complex was obtained in 70% yield (122.0 mg) as a black solid. ¹H NMR (400 MHz, MeOD) δ 8.90 – 8.84 (m, 2H), 8.81 (d, *J* = 6.5 Hz, 1H), 8.74 (dd, *J* = 15.5, 8.0 Hz, 4H), 8.53 (d, *J* = 7.7 Hz, 1H), 8.20 (t, *J* = 7.7 Hz, 3H), 8.16 – 8.10 (m, 4H), 8.06 (t, *J* = 7.6 Hz, 1H), 7.96 (d, *J* = 5.6 Hz, 2H), 7.92 (d, *J* = 5.5 Hz, 1H), 7.88 (d, *J* = 5.2 Hz, 1H), 7.83 (dd, *J* = 7.7, 5.8 Hz, 1H), 7.57 (dd, *J* = 14.0, 7.4 Hz, 2H), 7.44 (dt, *J* = 12.8, 6.4 Hz, 2H). HRMS (ESI) calcd for C₃₈H₂₅N₇ORu 348.5582 ([M]²⁺/2), found 348.5580 ([M]²⁺/2).

[Ru(phen)₂ASC]·(PF₆)₂ (2). With *cis*-[Ru(phen)₂Cl₂]·2H₂O (100.0 mg, 0.177 mmol, 1eq) in place of *cis*-[Ru(bpy)₂Cl₂]·2H₂O, this complex was obtained by a procedure similar to that described for complex **1**. This complex was obtained in 65% yield (119.0 mg) as a black solid. ¹H NMR (400 MHz, MeOD) δ 8.84 (t, *J* = 7.7 Hz, 2H), 8.77 – 8.69 (m, 5H), 8.54 (d, *J* = 8.2 Hz, 1H), 8.45 (t, *J* = 4.5 Hz, 2H), 8.37 – 8.30 (m, 4H), 8.15 – 8.03 (m, 6H), 7.86 (m, *J* = 13.5, 8.2, 5.3 Hz, 2H), 7.77 – 7.70 (m, 3H). HRMS (ESI) calcd for C₄₂H₂₅N₇ORu 372.5582 ([M]²⁺/2), found 372.5602 ([M]²⁺/2).

[Ru(tatp)₂ASC]·(PF₆)₂ (3). It was prepared by the same method as above one but starting from *cis*-[Ru(tatp)₂Cl₂]·2H₂O (119.0 mg, 0.177 mmol, 1eq) and ASC (50.0 mg, 0.177 mmol, 1eq). This complex was obtained in 52% yield (105.0 mg) as a black solid. ¹H NMR (400 MHz, DMSO) δ 9.64 – 9.52 (m, 1H), 9.40 (s, 1H), 8.97 (d, *J* = 8.2 Hz, 1H), 8.83 – 8.75 (m, 1H), 8.58 (d, *J* = 8.3 Hz, 1H), 8.47 (d, *J* = 5.4 Hz, 1H), 8.32 (dd, *J* = 5.3, 1.1 Hz, 1H), 8.26 (dd, *J* = 5.4, 1.1 Hz, 1H), 8.10 (m, *J* = 15.4, 13.7, 7.0, 3.3 Hz, 1H), 7.93 (m, *J* = 8.2, 6.9, 5.4 Hz, 1H), 7.74 (dd, *J* = 8.0, 5.6 Hz, 1H). HRMS (ESI) calcd for C₄₈H₂₅N₁₁ORu 424.5644 ([M]²⁺/2), found 424.5644 ([M]²⁺/2).

Physical measurements. ¹H NMR spectra were recorded on Varian Mercury-Plus 400 NMR instrument (¹H 400 MHz). Abbreviations for data quoted are s, singlet; d, doublet; t, triplet; dd, doublet of doublets; m, multiplet. Mass spectra were measured on an agilent TOF-G6230B mass spectrometer. FID (fluorescent intercalator displacement) measurements were recorded using an F-7000 fluorescence spectrophotometer (Hitachi Ltd., Japan) in a 1.0 cm path length quartz cuvette. Absorption spectra titrations were obtained by a UV-Vis (ultraviolet-visible) spectrophotometer (Hitachi U-3900). FRET (fluorescence resonance energy transfer) melting measurements were carried out on ABI-7500 real-time PCR (polymerase chain reaction) apparatus. UV-vis and FID

spectrophotometric measurements were carried out in buffer A and FRET melting measurements were performed in buffer B.

UV-Vis absorption titration. Initially, 3000 μL solutions of the blank buffer and the Ru complex sample (10 μM) were placed in the reference and sample cuvettes (1.0 cm path length), respectively, and then the first spectrum was recorded in the range of 200-600 nm. During the titration, an aliquot of buffered DNA solution (100 μM) was added to each cuvette to eliminate the absorbance of DNA itself, and the solutions were mixed by repeated inversion. Complex-DNA solutions were incubated for 5 min before absorption spectra were recorded. The titration processes were repeated until there was no change in the spectra for four titrations at least, indicating binding saturation had been achieved. The changes in the metal complex concentration due to dilution at the end of each titration were negligible.

The intrinsic binding constants K_b to DNA were determined based on the following equations (1) and (2) [52,76]:

$$(\varepsilon_a - \varepsilon_f) / (\varepsilon_b - \varepsilon_f) = (b - (b^2 - 2K^2 C_t [\text{DNA}] / s)^{1/2}) / 2KC_t \quad (1)$$

$$b = 1 + KC_t + K[\text{DNA}] / 2s \quad (2)$$

where $[\text{DNA}]$ is the concentration of DNA in base pairs, ε_a , ε_f , and ε_b are the apparent extinction coefficient $A_{\text{abs}}/[\text{M}]$, the extinction coefficient for the free metal (M) complex, and the extinction coefficient for the metal (M) complex in the fully bound form, respectively; K is the equilibrium binding constant in M^{-1} , C_t is the total metal complex concentration, and s is the binding size.

FID assay. To a mixture of the pre-folded G-quadruplex or duplex DNA (1 μM) and thiazole orange (TO) (2 μM), in a buffer A (100 mM), 10.0 μL corresponding compounds (200 μM) was added each time. After an equilibration time of 3 min the

emission spectrum was recorded between 500 and 650 nm with an excitation wavelength of 480 nm. The titration processes were repeated until there was no change in the spectra for at least four titrations, indicating that binding saturation had been achieved. The percentage of TO displacement is calculated using the following equation: percentage of displacement = $100 - [(F_t/F_0) \times 100]$, where F_t is the fluorescence intensity at each titration point and F_0 is the fluorescence of TO bound to DNA without any added complex as described earlier [70]. FID curves were obtained by plotting percentage of displacement versus concentration of complex. DC_{50} represents the amount of complex required to displace 50% of bound TO from a G-quadruplex.

FRET melting assay. The fluorescent double labeled oligonucleotides (5'-FAM-[DNA]-TAMRA-3'), (FAM: carboxyfluorescein, donor fluorophore, TAMRA: 6-carboxytetramethylrhodamine, acceptor fluorophore), used as the FRET probe was diluted in buffer B and then annealed by heating to 90 °C for 5 min, followed by slow cooling to room temperature, kept at 4 °C overnight. Double labeled DNAs were incubated with different concentrations of compounds for 1 h in the dark. The samples were prepared by aliquoting 10 μ L of the annealed DNA (0.25 μ M) into each strip, followed by 10 μ L of the compound solutions. Then, the strips were put into a PCR apparatus, and denaturation of oligonucleotides was performed using the following protocol: incubation at 25 °C for 2 min, and then increasing temperature to 95 °C in 0.5 °C increments, and the recording was performed after a 30 s stabilization to ensure a stable value. Measurements were made in triplicate with an excitation wavelength of 492 nm and emission wavelength of 516 nm, in a volume of 20 μ L for each sample. Final analysis of the data was carried out by using Origin Pro 8.5 data analysis. A DNA competition FRET melting assay was carried out to investigate the selectivity of the

compound to the quadruplex. All of the conditions of the experiment were similar to those used in the FRET melting assay, except that, added various concentrations of ds26 as competitors.

Molecular docking. Electronic structures of the compound were obtained in water using density functional theory (DFT) calculations. DFT calculations were carried out using Gaussian 09 by Becke's three parameter hybrid functional with the Lee-Yang-Parr correlation functional (B3LYP) methods. The geometries of compounds were optimized with the standard 6-311G** basis set for carbon, hydrogen, nitrogen, oxygen, while SDD basis set was used for Ru atom. The crystallographic structure of G-quadruplex DNA was down loaded from the Protein Data Bank (PDB) (<http://www.rcsb.org/pdb>). The 26-mer mixed parallel/antiparallel G-quadruplex structure in a K^+ solution (PDB ID: 2HY9) was used as the initial template for the docking studies. Before docking, necessary modifications were carried out according to a literature method [76]. Visualization of the docked molecules has been made with Accelrys Discovery Studio 2.5 software.

The molecular dynamic (MD) simulations were performed using GROMACS program. GROMOS force field GROMOS96 53A6 was introduced to the G-quadruplex before the energy minimization [77]. After a 1000 steps of energy minimization in vacuum, the G-quadruplex were placed in cubic box and the distance between the G-quadruplex and the box edge was set to be 1.0 nm, which could turn off the boundary effect of the system. The box was then filled with single point charge (SPC) water molecules, and 150 mM of sodium chloride was added to modify the ion condition and to neutralize the system. An energy-minimization in water with a steepest descent method for 3000 steps was carried out. The results of these minimizations produced the

starting structures for the MD simulations. The MD simulations were then carried out with a constant number of particles (N), pressure (P), and temperature (T), that is, NPT ensemble. The long-range electrostatic interactions were calculated by the Particle-Mesh Ewald (PME) method.

A constant pressure of 1 bar was applied with a coupling constant of 1.0 ps; G-quadruplex, water molecules, and ions were coupled separately to a bath at 310 K with a coupling constant of 0.1 ps. The equation of motion was integrated at each 2 fs time steps.

3. Results and discussion

Synthesis and characterization. Initially, the synthesis of the main ligand ASC requires the generation of the non-commercially available quinolone-5,8-dione in two steps. Sodium hydrogen sulfite reduction of available 5-nitro-8-hydroxyquinoline afforded 5-amino-8-hydroxyquinoline in moderate yield. 5-amino-8-hydroxyquinoline was converted into quinolone-5,8-dione in the presence of potassium dichromate under acidic conditions [72]. Then the synthesis of ASC was achieved mainly in three steps [68]. First of all, the alkyne building block was prepared from N-Boc-protected propargylamine and 2-iodoanilines by a Sonogashira coupling reaction, in good yield. Secondly, the oxidative amination between alkyne building block and quinoline-5,8-dione gives aminoquinone. And then, under an oxygen atmosphere, aminoquinone underwent the Brønsted Acid-Promoted Domino Cyclization to afford the ASC. Lastly, the coordination between the main ligand ASC and precursor complexes *cis*-[Ru(bpy)₂Cl₂] \cdot 2H₂O, *cis*-[Ru(phen)₂Cl₂] \cdot 2H₂O and *cis*-[Ru(tatp)₂Cl₂] \cdot 2H₂O afforded the product **1**, **2** and **3**, respectively. After further purification, the complexes were obtained with satisfactory purity and characterized by ¹H NMR and HRMS, details are

described in Fig. S1-S8. These compounds have a weak solubility in water, but have a high solubility in DMSO. Importantly, all complexes display remarkable stability in the buffered solution (10 mM Tris-HCl, 100 mM KCl buffer solution with pH value of 7.0, containing 1% DMSO) at 298 K for at least 3 days, as verified by UV-Vis spectroscopy (Fig. S9).

Absorption spectra titrations. UV absorption spectroscopy studies were carried out in order to investigate the binding affinity and binding mode of the compounds to G-quadruplex. As shown in Fig. 1, upon incremental additions of Htelo quadruplex to the corresponding compound solutions resulted in considerable hypochromicity of the intra-ligand charge transfer (ILCT) ($\lambda = 250\text{-}260$ nm) band and metal-to-ligand charge transfer (MLCT) ($\lambda = 400\text{-}420$ nm) band. A slight red shift was also observed. These features indicated strong interactions between complex **3** and ASC with DNA base pairs and $\pi\text{-}\pi$ stacking interactions between the aromatic regions of compounds and the G-quartets of the quadruplex. The spectra for complexes **1-2** are provided in Fig. S10. In order to compare the DNA binding affinities of these compounds to quadruplex, the intrinsic binding constants (K_b) were calculated by monitoring the changes of the MLCT absorbance. The intrinsic binding constants for complexes **1-3** and ASC were calculated to be $K_b = 2.78, 3.00, 3.12$ and $0.77 \times 10^6 \text{ M}^{-1}$, respectively. Such comparisons suggest that the trend in G-quadruplex DNA binding affinity is **3** > **2** > **1** > ASC, which indicates that complex **3** binds G-quadruplex more tightly than other compounds. The results are due to the different ancillary ligands. On going from bpy, phen to tatp, the plane area increase, leading to a greater DNA-binding affinity for complex **3**. Furthermore, the positive charges of Ru complexes are in favour of G-quadruplexes DNA binding, thus, all Ru complexes binds to DNA more strongly than

ASC does. Control experiments with ancillary ligands $[\text{Ru}(\text{L})_2\text{Cl}_2]$ ($\text{L} = \text{bpy}$, phen and tbp) were also performed (Fig. S11), as expected that these ligands have lower binding affinity than corresponding complexes **1-3**.

FID assay. We also utilized a FID assay to study interactions of these compounds with different sequences of DNA [78]. Four different DNA sequences were studied: three quadruplex forming sequences, namely, HTelo, c-myc and c-kit DNA and one duplex DNA (ds26) sequence. In our experiments, DNA was first treated with TO, yielding a fluorescent increase upon binding. Addition of the compounds results in a decrease of fluorescence intensity and finally quenched due to the displacement of TO from the DNA. The binding affinity of a small molecule for quadruplex and duplex DNA is determined by the DC_{50} value, which corresponds to the compound's concentration at which TO fluorescence decreases by 50%. Graphical representation of the TO displacement from quadruplex and duplex DNA for complexes **1-3** and ASC are shown in Fig. 2. Table 1 summarizes the DC_{50} values obtained from all FID assay. The DC_{50} value follows the order $\mathbf{3} < \mathbf{2} < \mathbf{1} < \text{ASC}$ for both quadruplex and duplex DNA. For all DNA sequences, low concentration of **3** was required to displace 50% TO, indicating that **3** is the strongest displacer and better G-quadruplex and duplex DNA binder than complexes **1-2** and ASC. FID results indicated that Ru complexes interact with both G-quadruplex and duplex DNA structures, showed lack of selectivity for different DNA structures. We also carried out the control experiments with ligands $[\text{Ru}(\text{L})_2\text{Cl}_2]$ ($\text{L} = \text{bpy}$, phen and tbp) (Fig. S12 and Table S1), results indicated that complexes **1-3** have more stronger binding ability for G-quadruplex and duplex DNA than corresponding ligands.

FRET melting assay. The stabilization ability of the compounds to G-quadruplex structures was investigated using FRET melting assay [52]. When the melting temperature increases, the quadruplexes structure opens up and the fluorophore and quencher move apart and fluorescence is restored. The emission of fluorescence was normalized between 0 and 1, and the T_m was defined as the melting temperature for which the normalized emission is 0.5 [52]. Compounds ability to stabilize G-quadruplex was determined by quantifying the change in melting temperature (ΔT_m) values. As summarized in Table 2, the melting temperature increase notably with different concentrations of compounds added into each quadruplex solution (except c-myc). As shown Fig. 3, upon treatment of the Htelo G-quadruplex (0.25 μM) with 3.5 μM complex **3** and ASC, ΔT_m values were 11.5 $^\circ\text{C}$ and 3 $^\circ\text{C}$, respectively. And for c-kit G-quadruplex, ΔT_m values were 11.0 $^\circ\text{C}$ and 4 $^\circ\text{C}$, respectively. The melting curves for complexes **1** and **2** are shown in Fig. S13. These results indicating that complex **3** is a more effective G-quadruplex stabilizer than complexes **1-2** and ASC, which is agreement with the above experimental results. The difference may originate from the different DNA-binding affinity.

The interaction of complexes **1-3** and ASC with the duplex DNA was also investigated. As depicted in Table 2, Fig. 3 and Fig. S13, complexes **1-2** and ASC were found to be no obvious stabilization effect for the ds26, ΔT_m values were 1 $^\circ\text{C}$, 0 $^\circ\text{C}$ and 2 $^\circ\text{C}$ induced by complexes **1-2** and ASC, respectively. Meanwhile, upon treatment of the ds26 with the same concentration of complex **3**, the melting temperature increased 7 $^\circ\text{C}$, indicating that complex **3** exhibits the strongest stabilization effects for duplex DNA.

A DNA competition FRET melting assay was also applied to explore the quadruplex versus duplex selectivity. More specifically, DNA competition FRET melting assay was

performed to show ΔT_m changes for a fixed concentration (3.5 μM) of added compound with G-quadruplex (Htelo, 0.25 μM) through the addition of increasing excess of duplex DNA (ds26). As shown in Fig. 4, using classical 5 and 15 μM competitor concentrations (equivalent to 20 and 60 times that of G-quadruplex), G-quadruplex melting temperature in the presence of complexes **1-3** and ASC is decreased dramatically, in comparison to the absence of this group of compounds, G-quadruplex stability significantly affected by the addition of excess amounts of ds26. These results indicate that complexes **1-3** and ASC are not selective for quadruplex versus duplex DNA and they can interact both quadruplex and duplex DNA. Control experiments with ligands $[\text{Ru}(\text{L})_2\text{Cl}_2]$ (L = bpy, phen and tatp) were also carried out, as summarized in Fig. S14-S15 and Table S2, these ligands have lower stabilizing ability to G-quadruplex and duplex DNA than corresponding complexes **1-3**.

Molecular docking. To elucidate the most favourable binding mode between the compounds and G-quadruplex DNA, molecular docking studies were carried out, which could corroborate the experimental results [70]. It has been reported that, small molecules potentially bind to a G-quadruplex by external stacking, intercalating between the quartets, or nonspecifically binding to the DNA strand [79]. And external stacking was the most potential binding mode for the many metal complexes and quadruplex. Our docking results revealed that, complexes **1-3** and ASC interact with mixed parallel/antiparallel G-quadruplex through an “external end-stacking” binding mode (results for all compounds are provided in Fig. S16-S17).

To further investigate these possible binding modes and get more reliable information, MD simulations and binding free energy calculations were carried out. MD simulation results suggested that similar external binding modes were achieved for complexes **1-3**

and ASC. It was also found that the binding modes between the complexes **1-3** and G-quadruplex DNA is a combination manner: π - π end stacking interactions (between the ligand and G-quartet), electrostatic interactions (between the metal and DNA's backbone) and hydrophobic effects. It is noteworthy that because of the combination binding mode of complex, it can bind well and tightly than the free ligand ASC. As shown in Fig. 5, complex **3** and ASC could stack on the both surfaces of the terminal G-quartet planes (5'- or 3' terminus) and the ligand preferred to stack on the center of a terminal G-quartet end with π - π stacking interactions, results for complexes **1-2** and ligands $[\text{Ru}(\text{L})_2\text{Cl}_2]$ (L = bpy, phen and tatp) are shown in Fig. S18-S19.

As summarized in Table. S3, the energetic differences between different poses were about 2-3 kcal·mol⁻¹. Due to the relatively larger π -aromatic contact surfaces and stronger ligand/DNA interactions, the lower binding free energy values (-12.8 kcal·mol⁻¹ for site-1 and -9.4 kcal·mol⁻¹ for site-2) were observed for complex **3** (Table. S4). These results were consistent with the spectral studies and confirmed again that complex **3** was the strongest binder.

Conclusions

To summarize, the act of conjugating a ASC ligands to a Ru(II) polypyridyl subunits resulted in a class of excellent DNA binders. A comparison of the DNA binding abilities of the free ASC ligand and the complexes, has revealed that the octahedral Ru(II) center played a crucial role in yielding good G-quadruplex and duplex DNA binders. Among three new complexes, complex **3** exhibited the strongest G-quadruplex and duplex DNA stabilization ability. Complex **3** was determined to be the most promising candidate for further in vitro studies and to be a potent anticancer drug. Though these complexes showed lack of selectivity for G-quadruplex over duplex DNA,

the present work provides the basis for the rational development of ASC derivatives as promising telomerase inhibitors and potential anticancer drugs.

Abbreviations

Ru	ruthenium
ASC	ascididemin
Htelo	human telomeric DNA
c-myc	cellular-myelocytomatosis viral oncogene
c-kit	oncogene c-kit promoter sequences
bcl-2	b-cell CLL/lymphoma 2
K-ras	kirsten rat sarcoma viral oncogene
UV-vis	ultraviolet-visible
FID	fluorescent intercalator displacement
FRET	fluorescence resonance energy transfer
MD	molecular dynamic
bpy	2,2'-bipyridine
phen	1,10-phenanthroline
tatp	1,4,8,9-tetra-aza-triphenylene
NAMI-A	imidazolium-trans-DMSO-imidazole-tetrachlororuthenate
KP1019	indazolium trans-[tetrachlorobis(1H-indazole)ruthenate(III)]
(N)KP1339	sodium trans-[tetrachloridobis(1H-indazole)ruthenate(III)]
tap	1,4,5,8-tetraazaphenanthrene
tpac	tetrapyridoacridine
dph	dipyrazino [2,3-a:2',3'-h]phenazine
FOA	4-(2,3- dihydroxypropyl)-formamide oxoaporphine

icip	2-(indeno[2,1-b]chromen-6-yl)-1H-imidazo[4,5-f][1,10]phenanthroline
pdppz	phenanthro[4,5-abc]dipyrido- [3,2-h:2',3'-j]phenazine
tactp	4,5,9,18-tetraazachryseno[9,10-b]-triphenylene
XPIP	X : Cl, PIP : 2-phenylimidazole[4, 5f][1,10]phenanthroline
bpibp	4, 4'-bis (1, 10-phenanthroline-[5, 6-d] imidazole-2-yl)-biphenyl
DMSO	dimethyl sulfoxide
EtOH	ethanol
MeCN	acetonitrile
MeOH	methanol
NMR	nuclear magnetic resonance spectroscopy
HRMS (ESI)	high resolution mass spectrometry (electrospray ionization)
PCR	polymerase chain reaction
TO	thiazole orange
DC ₅₀	half maximal displacement concentration
FAM	carboxyfluorescein
TAMRA	6-carboxytetramethylrhodamine
DFT	density functional theory
B3LYP	Becke's three parameter hybrid functional with the Lee-Yang-Parr correlation functional
PDB	protein data bank
SPC	single point charge
PME	Particle-Mesh Ewald
ILCT	intra-ligand charge transfer
MLCT	metal-to-ligand charge transfer

Acknowledgements

This work was supported by the National Natural Science Foundation of China (No. 21671150, 21877084, 81871730 and 21472139), Science and Technology Commission of Shanghai Municipality (No. 14DZ2261100) and the Fundamental Research Funds for the Central Universities.

References

- [1] M. A. Jakupec, M. Galanski, V. B. Arion, C. G. Hartinger, B. K. Keppler, Dalton Trans. 14 (2008) 183-194.
- [2] A.-M. Florea, D. Büsselberg, Cancers 3 (2011) 1351-1371.
- [3] M. J. Clarke, Coord. Chem. Rev. 236 (2003) 209-233.
- [4] H. Huang, P. Zhang, Y. Chen, K. Qiu, C. Jin, L. Ji, H. Chao, Dalton Trans. 45 (2016) 13135-13145.
- [5] P. J. Dyson, G. Sava, Dalton Trans. 16 (2006), 1929-1933.
- [6] J. M. Rademaker-Lakhai, D. V. D. Bongard, D. Pluim, J. H. Beijnen, J. H. M. Schellens, Clin. Cancer Res. 10 (2004) 3717-3727.
- [7] C. G. Hartinger, M. A. Jakupec, S. Zorbas-Seifried, M. Groessl, A. Egger, W. Berger, H. Zorbas, P. J. Dyson, B. K. Keppler, Chem. Biodivers. 5 (2008) 2140-2155.
- [8] A. K. Bytzek, G. Koellensperger, B. K. Keppler, C. G. Hartinger, J. Inorg. Biochem. 160 (2016) 250-255.
- [9] N. Shahabadi, S. Hadidi, Spectrochim. Acta. A. 96 (2012) 278-283.
- [10] Y.-J. Liu, C.-H. Zeng, H.-L. Huang, L.-X. He, F.-H. Wu, Eur. J. Med. Chem. 45 (2010) 564-571.

- [11] M. R. Gill, P. J. Jarman, S. Halder, M. G. Walker, H. K. Saeed, J. A. Thomas, C. Smythe, K. Ramadan, K. A. Vallis, *Chem. Sci.* 9 (2018) 841-849.
- [12] S. N. Georgiades, N. H. A. Karim, K. Suntharalingam, R. Vilar, *Angew. Chem. Int. Ed.* 49 (2010) 4020-4034.
- [13] Q. Cao, Y. Li, E. Freisinger, P. Z. Qin, R. K. O. Sigel, Z.-W. Mao, *Inorg. Chem. Front.* 4 (2017) 10-32.
- [14] M. R. Gill, J. A. Thomas, *Chem. Soc. Rev.* 41 (2012) 3179-3192.
- [15] D. Svozil, J. Kalina, M. Omelka, B. Schneider, *Nucleic Acids Res.* 36 (2008) 3690-3706.
- [16] T. J. Richmond, C. A. Davey, *Nature* 423 (2003) 145-150.
- [17] N. C. Seeman, H. Wang, X. Yang, F. Liu, C. Mao, W. Sun, L. Wenzler, Z. Shen, R. Sha, H. Yan, M. H. Wong, P. Sa-Ardyen, B. Liu, H. Qiu, X. Li, J. Qi, S. M. Du, Y. Zhang, J. E. Mueller, T.-J. Fu, Y. Wang, J. Chen, *Nanotechnology* 9 (1998) 257-273.
- [18] R. R. Sinden, Academic Press Sydney (1994).
- [19] A. H.-J. Wang, G. J. Quigley, F. J. Kolpak, J. L. Crawford, J. H. V. Boom, G. V. D. Marel, A. Rich, *Nature* 28 (1979) 680-686.
- [20] D. Bikard, C. Loot, Z. Baharoglu, D. Mazel, *Microbiol. Mol. Biol. Rev.* 74 (2010) 570-588.
- [21] L. Ying, M. I. Wallace, D. Klenerman, *Chem. Phys. Lett.* 334 (2001) 145-150.
- [22] K. R. Fox, T. Brown, *Biochem. Soc. Trans.* 39 (2011) 629-634.
- [23] M. Guéron, J.-L. Leroy, *Curr. Opin. Struct. Boil.* 10 (2000), 326-331.
- [24] M. L. Bochman, K. Paeschke, V. A. Zakian, *Nat. Rev. Genet.* 13 (2012), 770-780.
- [25] S. Bandeira, J. Gonzalez-Garcia, E. Pensa, R. Vilar, *Angew. Chem. Int. Ed.* 57 (2018) 310-313.

- [26] A. Shivalingam, M. A. Izquierdo, A. L. Marois, A. Vysniauskas, K. Suhling, M. K. Kuimova, R. Vilar, *Nat. Commun.* 6 (2015) 8178.
- [27] A. M. Zahler, J. R. Williamson, T. R. Cech, D. M. Prescott, *Nature* 350 (1991) 718-720.
- [28] L. Lu, M. Wang, L.-J. Liu, C.-H. Leung, D.-L. Ma, *ACS Appl. Mater. Inter.* 7 (2015) 8313-8318.
- [29] A. Zhao, C. Zhao, H. Tateishi-Karimata, J. Ren, N. Sugimoto, X. Qu, *Chem. Commun.* 52 (2016) 1903-1906.
- [30] K. E. Sitters, S. A. Sander, J. R. Devlin, J. R. Morrow, *Dalton Trans.* 44 (2015) 3708-3716.
- [31] A. Arola-Arnal, J. Benet-Buchholz, S. Neidle, R. Vilar, *Inorg. Chem.* 47 (2008) 11910-11919.
- [32] V. R. W. Harkness, A. K. Mittermaier, *BBA-Proteins and Proteomics* 1865 (2017) 1544-1554.
- [33] D. Rhodes, H. J. Lipps, *Nucleic Acids Res.* 43 (2015) 8627-8637.
- [34] B. Klejevska, A. L. B. Pyne, M. Reynolds, A. Shivalingam, R. Thorogate, B. W. Hoogenboom, L. Ying, R. Vilar, *Chem. Commun.* 52 (2016) 12454-12457.
- [35] J. L. Huppert, S. Balasubramanian, *Nucleic Acids Res.* 35 (2007) 406-413.
- [36] P. Murat, J. Zhong, L. Lekieffre, N. P. Cowieson, J. L. Clancy, T. Preiss, S. Balasubramanian, R. Khanna, J. Tellam, *Nat. Chem. Biol.* 10 (2014) 358-364.
- [37] K. W. Lim, V. C. M. Ng, N. Martín-Pintado, B. Heddi, A. T. Phan, *Nucleic Acids Res.* 41 (2013) 10556-10562.
- [38] C. Bazzicalupi, M. Ferraroni, F. Papi, L. Massai, B. Bertrand, L. Messori, P. Gratteri, A. Casini, *Angew. Chem. Int. Ed.* 55 (2016) 4256-4259.

- [39] J. Wang, Y. Chen, J. Ren, C. Zhao, X. Qu, *Nucleic Acids Res.* 42 (2014) 3792-3802.
- [40] J. E. Reed, A. A. Arnal, S. Neidle, R. Vilar, *J. Am. Chem. Soc.* 128 (2006) 5992-5993.
- [41] P. Phatak, J. C. Cookson, F. Dai, V. Smith, R. B. Gartenhaus, M. F. G. Stevens, A. M. Burger, *Br. J. Cancer* 96 (2007) 1223-1233.
- [42] I. Bessi, C. Bazzicalupi, C. Richter, H. R. A. Jonker, K. Saxena, C. Sissi, M. Chioccioli, S. Bianco, A. R. Bilia, H. Schwalbe, P. Gratteri, *ACS Chem. Biol.* 7 (2012) 1109-1119.
- [43] Q. Wang, J.-Q. Liu, Z. Chen, K.-W. Zheng, C.-Y. Chen, Y.-H. Hao, Z. Tan, *Nucleic Acids Res.* 39 (2011) 6229-6237.
- [44] D.-L. Ma, Z. Zhang, M. Wang, L. Lu, H.-J. Zhong, C.-H. Leung, *Chem. Biol.* 22 (2015) 812-828.
- [45] L. Xu, X. Chen, J. Wu, J. Wang, L. Ji, H. Chao, *Chem. Eur. J.* 21 (2015) 4008-4020.
- [46] S. Cogoi, L. E. Xodo, *Nucleic Acids Res.* 34 (2006) 2536-2549.
- [47] K. E. Erkkila, D. T. Odom, J. K. Barton, *Chem. Rev.* 99 (1999) 2777-2795.
- [48] A. C. Komor, J. K. Barton, *Chem. Commun.* 49 (2013) 3617-3630.
- [49] B. Onfelt, P. Lincoln, B. Nordén, *J. Am. Chem. Soc.* 123 (2001), 3630-3637.
- [50] L.-N. Ji, X.-H. Zou, J.-G. Liu, *Coord. Chem. Rev.* 216 (2001) 513-536.
- [51] J.-L. Yao, X. Gao, W. Sun, S. Shi, T.-M. Yao, *Dalton Trans.* 42 (2013) 5661-5672.
- [52] S. Shi, J.-H. Xu, X. Gao, H.-L. Huang, T.-M. Yao, *Chem. Eur. J.* 21 (2015) 11435-11445.
- [53] S. Shi, J. Liu, T. Yao, X. Geng, L. Jiang, Q. Yang, L. Cheng, L. Ji, *Inorg. Chem.* 47 (2008) 2910-2912.

- [54] S. Shi, H.-L. Huang, X. Gao, J.-L. Yao, C.-Y. Lv, J. Zhao, W.-L. Sun, T.-M. Yao, L.-N. Ji, *J. Inorg. Biochem.* 121 (2013) 19-27.
- [55] S. Rickling, L. Ghisdavu, F. Pierard, P. Gerbaux, M. Surin, P. Murat, E. Defrancq, C. Moucheron, A. K.-D. Mesmaeker, *Chem. Eur. J.* 16 (2010) 3951-961.
- [56] G. Piraux, L. Bar, M. Abraham, T. Lavergne, H. Jamet, J. Dejeu, L. Marcélis, E. Defrancq, B. Elias, *Chem. Eur. J.* 23 (2017) 11872-1880.
- [57] Z.-F. Chen, Q.-P. Qin, J.-L. Qin, J. Zhou, Y.-L. Li, N. Li, Y.-C. Liu, H. Liang, *J. Med. Chem.* 58 (2015) 4771-4789.
- [58] G. Liao, X. Chen, J. Wu, C. Qian, Y. Wang, L. Ji, H. Chao, *Dalton Trans.* 44 (2015) 15145-15156.
- [59] Q. Wu, K. Zheng, S. Liao, Y. Ding, Y. Li, W. Mei, *Organometallics* 35 (2016) 317-326.
- [60] C. Zheng, Y. Liu, Y. Liu, X. Qin, Y. Zhou, J. Liu, *J. Inorg. Biochem.* 156 (2016) 122-132.
- [61] G. Minotti, P. Menna, E. Salvatorelli, G. Cairo, L. Gianni, *Pharmacol Rev.* 56 (2004) 185-229.
- [62] J. Ren, J. B. Chaires, *Biochemistry* 38 (1999) 16067-16075.
- [63] D. A. Gewirtz, *Biochem. Pharmacol.* 57 (1999) 727-741.
- [64] G. G. Hu, X. Shui, F. Leng, W. Priebe, J. B. Chaires, L. D. Williams, *Biochemistry* 36 (1997) 5940-5946.
- [65] A. H.-J. Wang, G. Ughetto, G. J. Quigley, A. Rich, *Biochemistry* 26 (1987) 1152-1163.
- [66] L. Dassonneville, N. Wattez, B. Baldeyrou, C. Mahieu, A. Lansiaux, B. Banaigs, I. Bonnard, C. Bailly, *Biochem. Pharmacol.* 60 (2000) 527-537.

- [67] D. Skyle, C. H. Heathcock, *J. Nat. Prod.* 65 (2002) 1573-1581.
- [68] H. Yin, N. Shan, S. Wang, Z.-J. Yao, *J. Org. Chem.* 79 (2014) 9748-9753.
- [69] I. Bonnard, N. Bontemps, S. Iahmy, B. Banaigs, G. Combaut, C. Francisco, P. Colson, C. Houssier, M. Waring, C. Bailly, *Anticancer Drug Des.* 10 (1995), 333-346.
- [70] S. Shi, X. Gao, H. Huang, J. Zhao, T. Yao, *Chem. Eur. J.* 21 (2015) 13390-13400.
- [71] C. R. Cantor, M. M. Warshaw, H. Shapiro, *Biopolymers* 9 (1970) 1059-1077.
- [72] M. Paige, G. Kosturko, G. Bulut, M. Miessau, S. Rahim, J. A. Toretzky, M. L. Brown, A. Üren, *Bioorg. Med. Chem.* 22 (2014) 478-487.
- [73] W. Paw, R. Eisenberg, *Inorg. Chem.* 36 (1997) 2287-2293.
- [74] J. Bolger, A. Gourdon, E. Ishow, J.-P. Launay, *Inorg. Chem.* 35 (1996) 2937-2944.
- [75] B. P. Sullivan, D. J. Salmon, T. J. Meyer, *Inorg. Chem.* 17 (1978) 3334-3341.
- [76] X.-H. Lu, S. Shi, J.-L. Yao, H.-L. Huang, T.-M. Yao, *J. Inorg. Biochem.* 140 (2014) 64-71.
- [77] S. Pronk, S. Páll, R. Schulz, P. Larsson, P. Bjelkmar, R. Apostolov, M. R. Shirts, J. C. Smith, P. M. Kasson, D. V. D. Spoel, B. Hess, E. Lindahl, *Bioinformatics* 29 (2013) 845-854.
- [78] D. Monchaud, C. Allain, H. Bertrand, N. Smargiasso, F. Rosu, V. Gabelica, A. D. Cian, J.-L. Mergny, M.-P. Teulade-Fichou, *Biochimie* 90 (2008) 1207-1223.
- [79] E. S. Baker, J. T. Lee, J. L. Sessler, M. T. Bowers, *J. Am. Chem. Soc.* 128 (2006) 2641-2648.

Figure Captions

Scheme 1 Synthetic route to $[\text{Ru}(\text{bpy})_2\text{ASC}]^{2+}$ (**1**), $[\text{Ru}(\text{phen})_2\text{ASC}]^{2+}$ (**2**), $[\text{Ru}(\text{tstp})_2\text{ASC}]^{2+}$ (**3**).

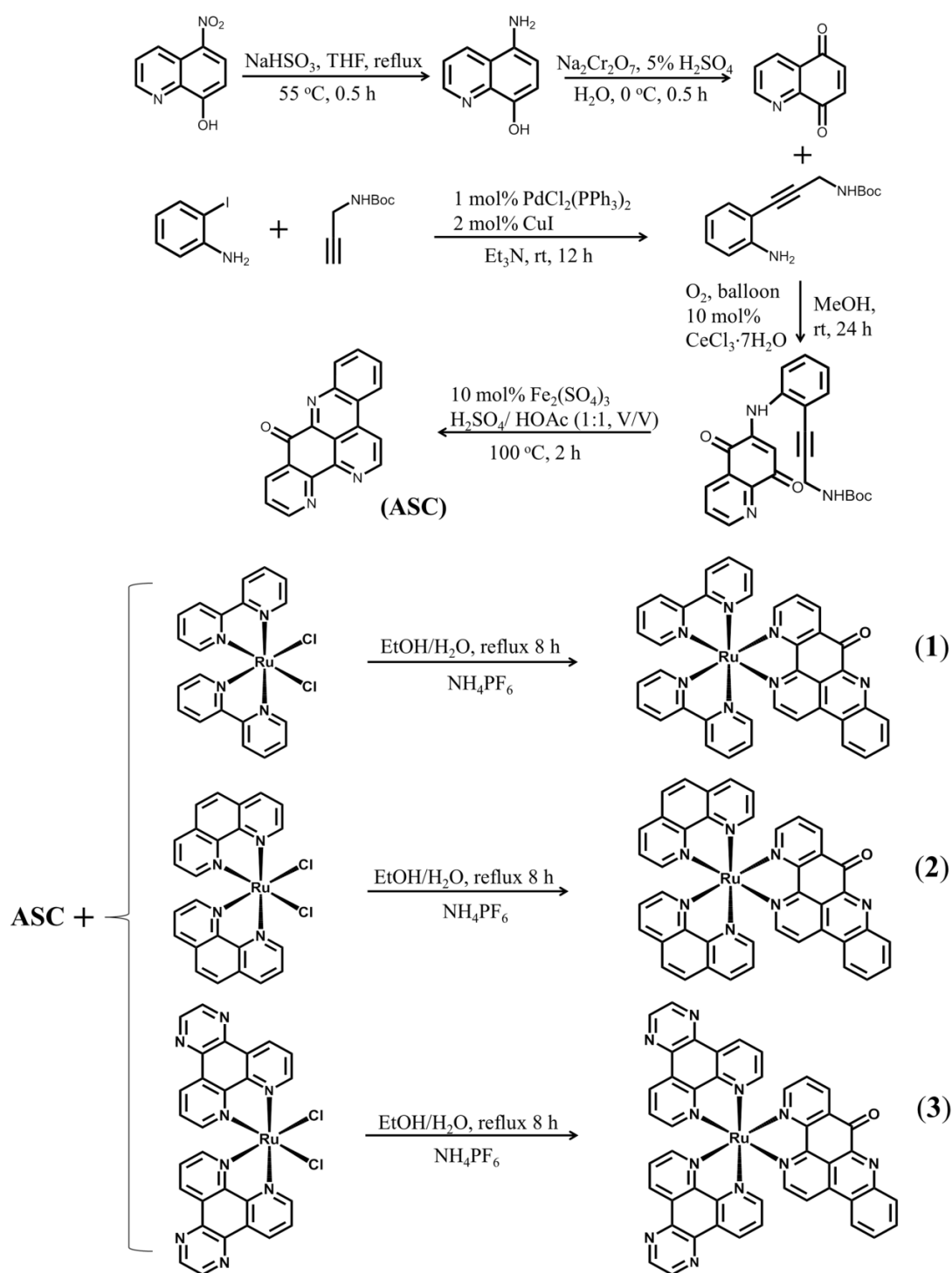
Fig. 1 Absorption spectra of $[\text{Ru}(\text{tstp})_2\text{ASC}]^{2+}$ (**3**) (A) and ASC (B) ($10 \mu\text{M}$) titration by G-quadruplex DNA in presence of Htelo in 10 mM Tris-HCl, 100 mM KCl buffer, pH=7.0, $[\text{DNA}]=(0-15 \mu\text{M})$. Inset: plots of $(\epsilon_a-\epsilon_f)/(\epsilon_b-\epsilon_f)$ vs $[\text{DNA}]$.

Fig. 2 Graphical representation of the TO ($2 \mu\text{M}$) displacement from Htelo (A), c-kit (B), c-myc (C) G-quadruplexes and ds26 (D) duplex DNA ($1 \mu\text{M}$) upon increasing concentration of complexes **1-3** and ASC.

Fig. 3 Normalized FRET melting curves of G-quadruplex and duplex (ds26) DNA ($0.25 \mu\text{M}$) in K^+ buffer, with increasing concentrations ($0-3.5 \mu\text{M}$) of $[\text{Ru}(\text{tstp})_2\text{ASC}]^{2+}$ (**3**) (A-D) and ASC (E-H) measured by real-time PCR system.

Fig. 4 Competitive FRET-melting curves of Htelo ($0.25 \mu\text{M}$) with $3.5 \mu\text{M}$ of $[\text{Ru}(\text{bpy})_2\text{ASC}]^{2+}$ (**1**) (A), $[\text{Ru}(\text{phen})_2\text{ASC}]^{2+}$ (**2**) (B), $[\text{Ru}(\text{tstp})_2\text{ASC}]^{2+}$ (**3**) (C), ASC (D) and duplex competitor ds26 ($5-15 \mu\text{M}$) in buffer containing 100 mM KCl.

Fig. 5 The calculated model of the compounds bind to the mixed hybrid type G-quadruplex DNA at site-1 and site-2 (A) $[\text{Ru}(\text{tstp})_2\text{ASC}]^{2+}$ (**3**), (B) ASC.



Scheme 1 Synthetic route to [Ru(bpy)₂ASC]²⁺ (1), [Ru(phen)₂ASC]²⁺ (2), [Ru(tatp)₂ASC]²⁺ (3).

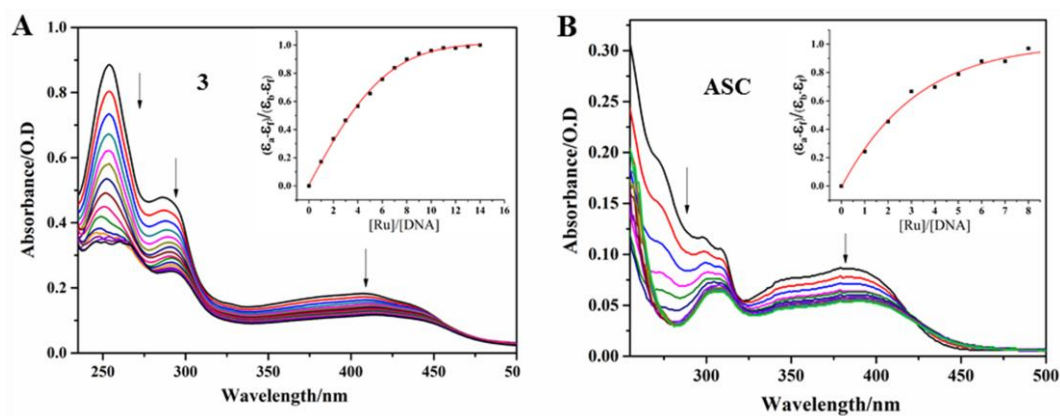


Fig. 1. Absorption spectra of $[\text{Ru}(\text{tatp})_2\text{ASC}]^{2+}$ (**3**) (A) and ASC (B) ($10 \mu\text{M}$) titration by G-quadruplex DNA in presence of Htelo in 10 mM Tris-HCl , 100 mM KCl buffer, $\text{pH}=7.0$, $[\text{DNA}]=(0-15 \mu\text{M})$. Inset: plots of $(\epsilon_a-\epsilon_f)/(\epsilon_b-\epsilon_f)$ vs $[\text{DNA}]$.

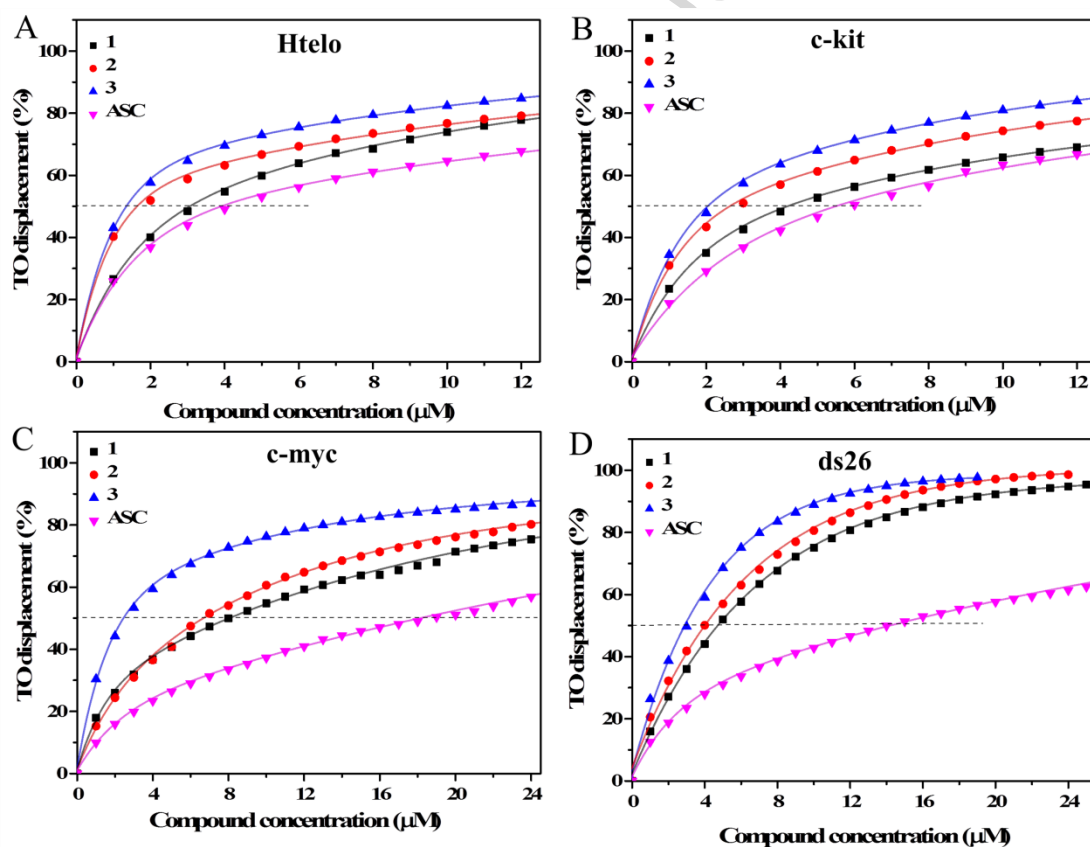


Fig. 2. Graphical representation of the TO ($2 \mu\text{M}$) displacement from Htelo (A), c-kit (B), c-myc (C) G-quadruplexes and ds26 (D) duplex DNA ($1 \mu\text{M}$) upon increasing concentration of complexes **1-3** and ASC.

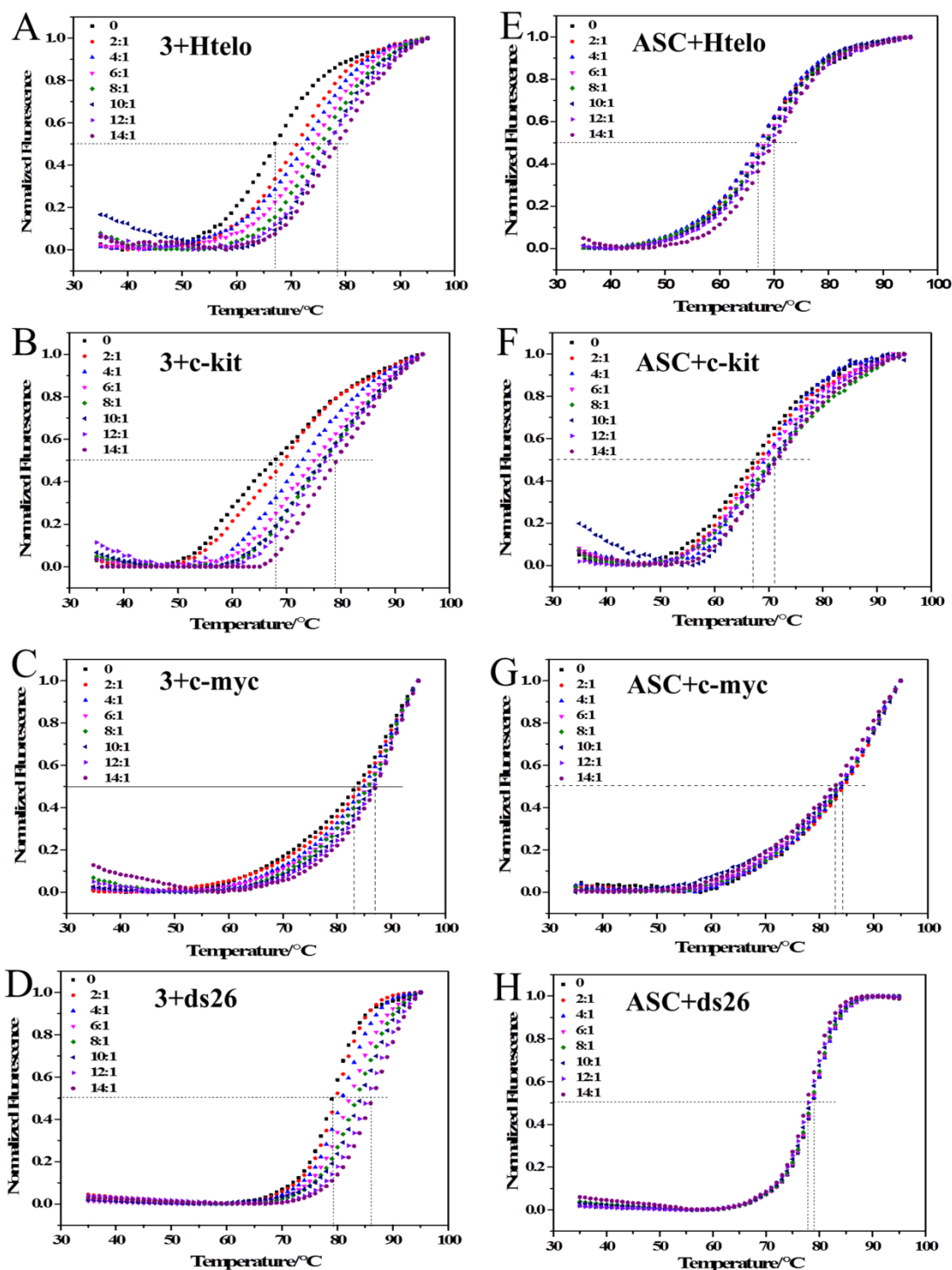


Fig. 3. Normalized FRET melting curves of G-quadruplex and duplex (ds26) DNA (0.25 μM) in K^+ buffer, with increasing concentrations (0-3.5 μM) of $[\text{Ru}(\text{tatp})_2\text{ASC}]^{2+}$ (3) (A-D) and ASC (E-H) measured by real-time PCR system.

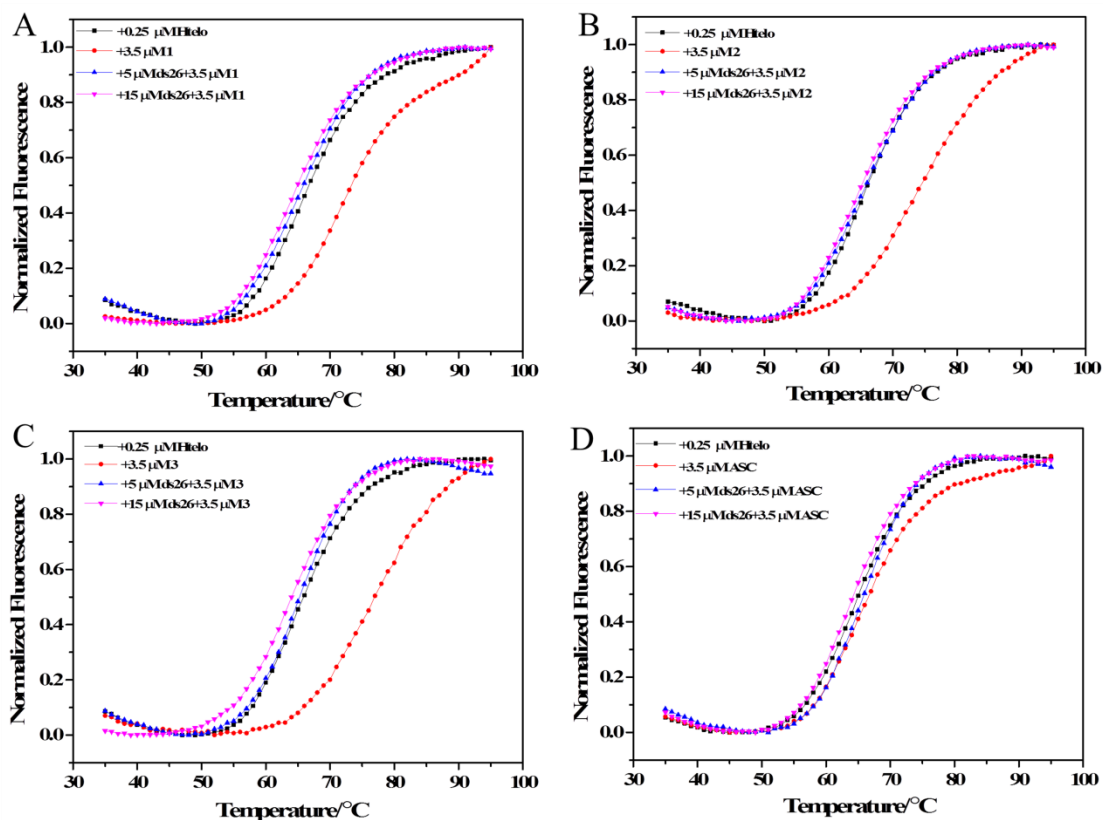


Fig. 4. Competitive FRET-melting curves of Htelo (0.25 μM) with 3.5 μM of [Ru(bpy)₂ASC]²⁺ (1) (A), [Ru(phen)₂ASC]²⁺ (2) (B), [Ru(tatp)₂ASC]²⁺ (3) (C), ASC (D) and duplex competitor ds26 (5-15 μM) in buffer containing 100 mM KCl.

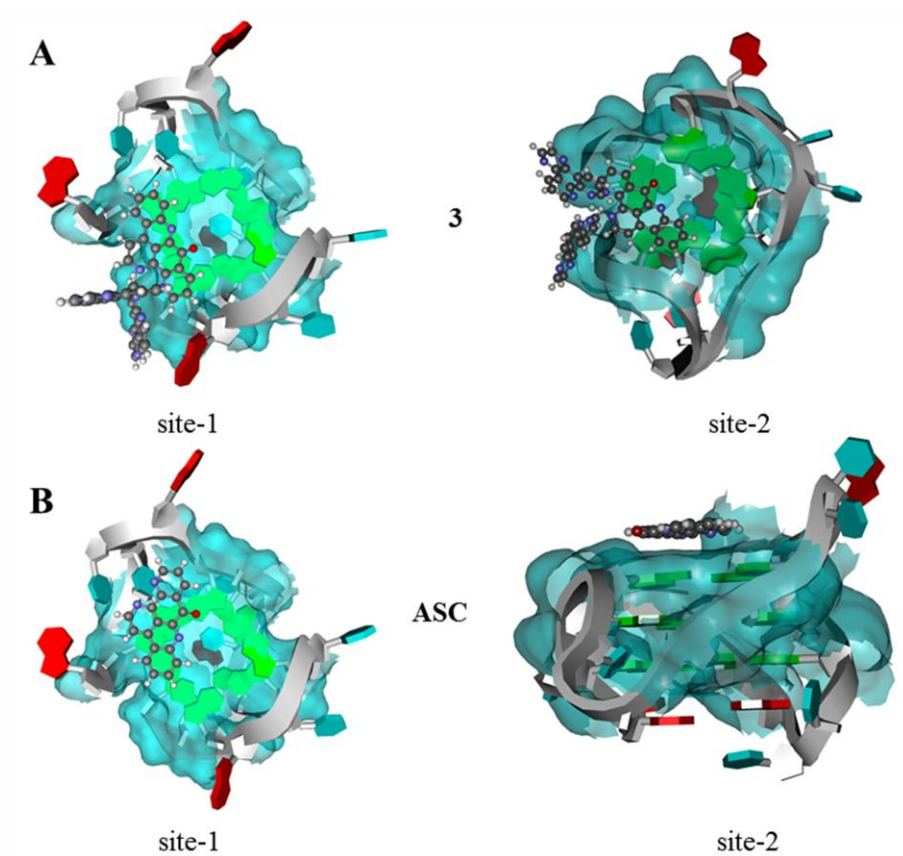


Fig. 5. MD simulation of the $[\text{Ru}(\text{tatp})_2\text{ASC}]^{2+}$ (**3**) (A) and ASC (B) bind to the mixed hybrid type G-quadruplex DNA at site-1 and site-2.

Table 1

$H_{telo}DC_{50}$, $c\text{-kit}DC_{50}$, $c\text{-myc}DC_{50}$ and $ds^{26}DC_{50}$ values (μM) determined by FID assay for complexes **1-3** and ASC.

Compound	TO displacement (μM)				Selectivity		
	$H_{telo}DC_{50}$	$c\text{-kit}DC_{50}$	$c\text{-myc}DC_{50}$	$ds^{26}DC_{50}$	$ds^{26}DC_{50}/H_{telo}DC_{50}$	$ds^{26}DC_{50}/c\text{-kit}DC_{50}$	$ds^{26}DC_{50}/c\text{-myc}DC_{50}$
1	3.16	4.31	8.36	4.87	1.54	1.13	0.57
2	1.68	2.71	6.93	4.01	2.39	1.48	0.58
3	1.33	2.04	2.42	3.00	2.26	1.47	1.24
ASC	4.15	5.62	18.44	14.88	3.59	2.65	0.81

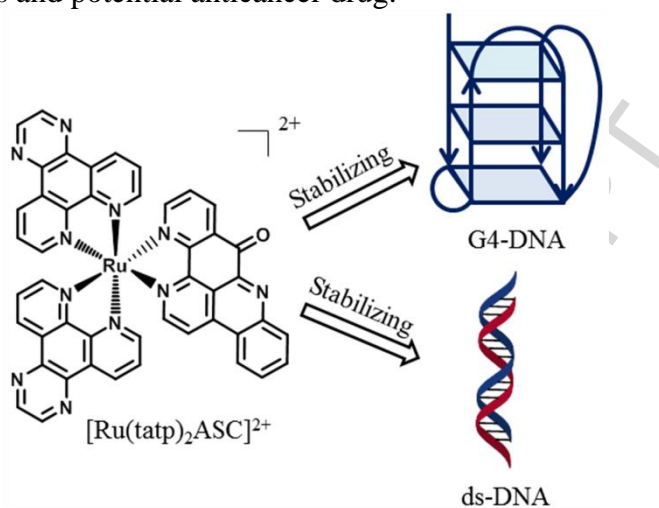
Table 2

Stabilization effect of complexes **1-3** and ASC (3.5 μM) on different types of G-quadruplexes and duplex DNA (0.25 μM).

Compound	$H_{telo}/^{\circ}\text{C}$	$c\text{-kit}/^{\circ}\text{C}$	$c\text{-myc}/^{\circ}\text{C}$	$ds^{26}/^{\circ}\text{C}$
1	8	6	2	0
2	10	8	3	2
3	11.5	11	4	7
ASC	3	4	1	1

Graphical abstract

The act of conjugating ascididemin (ASC) ligands to a Ru(II) polypyridyl subunits resulted in a class of excellent DNA binders. Especially, [Ru(1,4,8,9-tetra-aza-triphenylene)₂ASC]·(PF₆)₂ (**3**) showed the strongest quadruplex and duplex DNA binding and stabilization ability. Complex **3** was proposed to be the promising telomerase inhibitors and potential anticancer drug.



ACCEPTED MAN

Highlights

- (1) Three novel Ru(II) polypyridyl complexes have been synthesized and characterized.
- (2) Complexes **1-3** and ascididemin (ASC) can effectively bind G-quadruplex and duplex DNA.
- (3) Notably, complex **3** exhibited the strongest DNA binding and stabilization ability.
- (4) Complex **3** was determined to be the most promising candidate for further in vitro studies.
- (5) Complex **3** is $[\text{Ru}(1,4,8,9\text{-tetra-aza-triphenylene})_2\text{ASC}] \cdot (\text{PF}_6)_2$.